Published OnlineFirst December 15, 2014; DOI: 10.1158/0008-5472.CAN-14-0839

Therapeutics, Targets, and Chemical Biology

Cancer Research

BRCA2-Deficient Sarcomatoid Mammary Tumors Exhibit Multidrug Resistance

Janneke E. Jaspers[1,2], Wendy Sol[1], Ariena Kersbergen[1], Andreas Schlicker[3], Charlotte Guyader[1], Guotai Xu[1], Lodewyk Wessels[3], Piet Borst[1], Jos Jonkers[2], and Sven Rottenberg[1,4]

Abstract

Pan- or multidrug resistance is a central problem in clinical oncology. Here, we use a genetically engineered mouse model of BRCA2-associated hereditary breast cancer to study drug resistance to several types of chemotherapy and PARP inhibition. We found that multidrug resistance was strongly associated with an EMT-like sarcomatoid phenotype and high expression of the *Abcb1b* gene, which encodes the drug efflux transporter P-glycoprotein. Inhibition of P-glycoprotein could partly resensitize sarcomatoid tumors to the PARP inhibitor olaparib, docetaxel, and doxorubicin. We propose that multidrug resistance is a multifactorial process and that mouse models are useful to unravel this. *Cancer Res; 75(4); 732–41. ©2014 AACR.*

Introduction

A major clinical problem in cancer therapy is resistance of tumors to all available therapies, a phenomenon called pan-resistance (1). After an initial response primary tumors and especially metastases do not respond anymore to treatment, including radiotherapy. The frequently used term "multidrug resistance" historically refers to resistance due to drug efflux transporters, but upregulation of these transporters cannot fully explain pan-resistance. Drug resistance is not only a problem for classical chemotherapeutics, but also for targeted therapeutics. Mechanisms can be drug-specific, such as imatinib resistance caused by mutations in or overexpression of the drug target BCR–ABL (2), or downregulation of *Top1* or *Top2* causing resistance to topoisomerase I or II poisons (3). The precise mechanisms that cause resistance of tumors to multiple classes of drugs are not fully understood. One mechanism that has been put forward to explain pan-resistance of various types of cancer is epithelial-to-mesenchymal transition (EMT; refs. 1, 4). During EMT cells lose epithelial characteristics and acquire mesenchymal characteristics. EMT is a physiologic process involved in, for example, embryogenesis and wound healing, but it has also been described for epithelial cancers when cells acquire a spindle-shaped (also called "mesenchymal" or "sarcomatoid") morphology and lose expression of cell adhesion molecules. *In vitro*, EMT was observed in various cell lines that acquired resistance to chemotherapeutic agents and targeted inhibitors (4), and induction of EMT by recombinant TGFβ treatment led to resistance to tyrosine kinase inhibitors and cisplatin (5), suggesting a role of EMT in pan-resistance.

Breast cancer is a heterogeneous disease, which comprises various histologic and molecular subtypes. Among these is the subgroup of metaplastic breast cancer, a variant of triple-negative breast cancer, which includes several morphologic entities, including spindle-shaped tumor cells (6, 7). A molecular subtype that is frequently observed in metaplastic cancers is the claudin-low signature (8, 9). Because metaplastic cancers have a poor prognosis, we wondered whether EMT might contribute to poor drug response of these tumors.

To study the influence of EMT on pan-resistance, we made use of a unique mouse model of BRCA2-deficient breast cancer, that is, the *K14cre;Brca2*$^{F/F}$*;p53*$^{F/F}$ mammary tumor model (10). Female *K14cre;Brca2*$^{F/F}$*;p53*$^{F/F}$ mice develop mostly epithelial mammary carcinomas, but also mesenchymal carcinosarcomas are formed. Because the K14 promoter drives Cre expression only in epithelial cells (10), it is plausible that these mesenchymal mammary tumors originate from an EMT. The advantage of such an *in vivo* model is that no cell lines have to be used, which may poorly represent the original tumor (11). We and others have previously shown that the BRCA2-deficient mouse mammary tumors are sensitive to DNA damage–inducing drugs and PARP inhibitors due to the lack of error-free repair of double-strand DNA breaks by homologous recombination (12–16). In patients with BRCA2-deficient breast cancer, such an increased sensitivity was also observed after neoadjuvant therapy with DNA-damaging agents (17, 18) or PARP inhibitors (19). We investigated whether this drug sensitivity is diminished in BRCA2-deficient carcinosarcomas. For this purpose, we compared the responses of epithelial carcinomas and mesenchymal carcinosarcomas with chemotherapy drugs and PARP inhibitors. We found that BRCA2-deficient carcinosarcomas are multidrug resistant, which was, at least in part, due to high expression of the drug efflux transporters P-glycoprotein (Pgp) and breast cancer resistance protein (BCRP), which transport a wide range of chemotherapeutic and targeted agents. In addition, we found that an EMT-like gene-expression

[1]Division of Molecular Oncology, Netherlands Cancer Institute, Amsterdam, the Netherlands. [2]Division of Molecular Pathology, Netherlands Cancer Institute, Amsterdam, the Netherlands. [3]Division of Molecular Carcinogenesis, Netherlands Cancer Institute, Amsterdam, the Netherlands. [4]Institute of Animal Pathology, Vetsuisse Faculty, University of Bern, Bern, Switzerland.

Note: Supplementary data for this article are available at Cancer Research Online (http://cancerres.aacrjournals.org/).

Corresponding Author: Sven Rottenberg, Institute of Animal Pathology, Vetsuisse Faculty, University of Bern, Laenggassstr. 122, 3012 Bern, Switzerland. Phone: 41-31-6312395; E-mail: sven.rottenberg@vetsuisse.unibe.ch

doi: 10.1158/0008-5472.CAN-14-0839

©2014 American Association for Cancer Research.

Downloaded from cancerres.aacrjournals.org on September 22, 2019. © 2015 American Association for Cancer Research.

Published OnlineFirst December 15, 2014; DOI: 10.1158/0008-5472.CAN-14-0839

profile correlates with Pgp expression in multiple independent mouse mammary tumor datasets.

Materials and Methods

Mice and tumor transplantations

Tumors were generated in *K14cre;Brca2*$^{F/F}$;*p53*$^{F/F}$ (KB2P) female mice (10) and samples were taken for histology, RNA isolation and cryopreservation. Orthotopic transplantation of *Brca2*$^{\Delta/\Delta}$; *p53*$^{\Delta/\Delta}$, *p53*$^{\Delta/\Delta}$, and *p53*$^{\Delta/\Delta}$;*Abcb1a/b*$^{-/-}$ tumors in wild-type FVB/Ola129 F1 mice was performed as previously described (20). The tumor size was monitored at least three times a week by calliper measurements. The tumor volume was calculated with the following formula: 0.5 × length × width^2. Animals were sacrificed with CO_2, when the tumor reached a size of 1,500 mm^3. Cre-mediated deletion of exon 11 in *Brca2* and exons 2–10 in *Trp53* was confirmed by genotyping PCR and Southern blotting as described previously (14, 21). All animal experiments were approved by the Animal Ethics Committee of the Netherlands Cancer Institute (Amsterdam, the Netherlands).

Drug treatments

Upon tumor outgrowth to approximately 200 mm^3 (100%) the mice were either left untreated or received one of the following treatments: olaparib (50 mg/kg i.p., daily for 28 days), topotecan (4 mg/kg i.p., days 0–4 and days 14–18), doxorubicin (Amersham Pharmacia Netherlands; 5 mg/kg i.v., days 0, 7, and 14), docetaxel (Aventis; 25 mg/kg i.v., days 0, 7, and 14) or cisplatin (Mayne Pharma; 6 mg/kg i.v., day 0). Mice with a relapsing tumor received another treatment cycle when the tumor was 100% of the original size at treatment start. For the resensitization experiment with tariquidar (Fig. 4B), the mice received only one treatment cycle and tumor outgrowth was monitored. Tariquidar (Avaant; 10 mg/kg i.p.) was administered 15 minutes before treatment with olaparib, docetaxel, or doxorubicin. AZD2461 (100 mg/kg orally; ref. 22) was administered daily for 28 days.

Immunohistochemistry and fluorescence

Staining of E-cadherin and vimentin was performed on formalin-fixed paraffin-embedded (FFPE) tissue. Samples were boiled in Tris-EDTA pH9.0 to retrieve the antigens. Furthermore, we used 3% H_2O_2 in methanol to block endogenous peroxidase activity, and 10% milk (E-cadherin) or 4% BSA plus 5% normal goat serum in PBS (vimentin) as blocking buffer. Primary antibodies (mouse anti–E-cadherin, BD Transduction Laboratories 610182, 1:400; rabbit anti-vimentin, Cell Signaling Technology 5741, 1:200) were diluted in 1.25% normal goat serum plus 1% BSA in PBS. For detection and visualization labeled polymer-HRP (horseradish peroxidase) anti-mouse and rabbit Envision (Dako K4007 and K4011), DAB (Sigma D5905), and hematoxylin counterstaining were applied.

CD31 staining was done on cryosections after acetone fixation for 10 minutes at −20°C. Then we applied 0.3% H_2O_2 in methanol, avidin–biotin block (Dako X0590) and serum-free protein block (Dako X0909). The primary (rat anti-CD31, BD Biosciences 550274; 1:1,000) and secondary antibodies (biotinylated rabbit-anti–rat IgG, Dako E0468, 1:300) were diluted in 1% BSA in PBS. For detection and visualization, we used streptavidin–HRP (Dako K1016, 10 minutes incubation at room temperature), DAB (Dako K3468), and hematoxylin counterstaining.

For visualization of perfused blood vessels, biotinylated Lycopersicon Esculentum (Tomato) Lectin (B1175 Vector Laboratories) was added to streptavidin-AF633 (S21375 Invitrogen) in sterile PBS and injected in the tail vein 15 minutes before sacrificing the mouse. For visualization of the Lectin-AF633 signal, FFPE slides were deparaffinized, rehydrated, incubated with DAPI for 5 minutes, and mounted in Vectashield (H-1000 Vector Laboratories). Images were taken with a Leica TCS SP5 (Leica Microsystems) confocal system, equipped with a 405-nm Diode laser and 633-nm HeNe laser system.

Gene-expression profiling

Total RNA was isolated with TRIzol (Invitrogen) from snap-frozen tumor samples. The RNA was processed according to the manufacturer's instructions for single channel 45K MouseWG-6 v2.0 BeadChips (Illumina). Background correction was performed using the bg.adjust method from the Bioconductor affy package (23). For normalization between arrays, the robust spline method was applied.

EMT signature and EMT score

A published EMT signature (5) was converted from human to mouse, resulting in 239 epithelial genes (down after EMT) and 224 mesenchymal genes (up after EMT). Of these, 235 epithelial and 223 mesenchymal genes could be mapped to Ensembl gene identifiers using Ensembl Biomart (24).

Generation of gene-expression data from *p53*$^{\Delta/\Delta}$ and *Cdh1*$^{\Delta/\Delta}$; *p53*$^{\Delta/\Delta}$ mouse mammary tumors has been described (Klijn and colleagues; submitted for publication). Gene-expression datasets GSE3165 (25), GSE23938 (26), and GSE10885 (27) were downloaded from the Gene Expression Omnibus.

Expression data were mean-centered per gene or probe for each dataset. The EMT score of each tumor in all datasets is calculated by subtracting the mean $\log_2$ expression of the epithelial genes from the mean of the $\log_2$ expression of the mesenchymal genes. Supplementary Table S1 summarizes the number of signature genes represented on each platform. As a result, tumors with a mesenchymal gene-expression profile have a positive score and tumors with an epithelial profile have a negative EMT score. For the correlation between EMT score and *Abcb1a*, *Abcb1b*, and *Abcg2* expressions, we used the Spearman correlation and significance was tested with the *t* distribution test.

Array comparative genomic hybridization

Array comparative genomic hybridization (aCGH) data from *Brca2*$^{\Delta/\Delta}$;*p53*$^{\Delta/\Delta}$ mouse mammary tumors were downloaded from Array Express (E-NCMF-34 and E-NCMF-35). The phenotype was determined previously (28), with one exception: a tumor with unknown phenotype was later classified as carcinosarcoma. Unsupervised hierarchical clustering was performed using the Euclidean distance method with complete linkage.

RT-MLPA

Semiquantitative levels of *Abcb1a*, *Abcb1b*, and *Abcg2* mRNA were measured with reverse transcriptase multiplex ligation–dependent probe amplification (RT-MLPA). Reverse transcription of total RNA, hybridization, ligation, PCR amplification, and fragment analysis by capillary electrophoresis were performed as described previously (29). Gene-expression levels were normalized to the internal reference *Actb* (β-actin).

Downloaded from cancerres.aacrjournals.org on September 22, 2019. © 2015 American Association for Cancer Research.

Published OnlineFirst December 15, 2014; DOI: 10.1158/0008-5472.CAN-14-0839

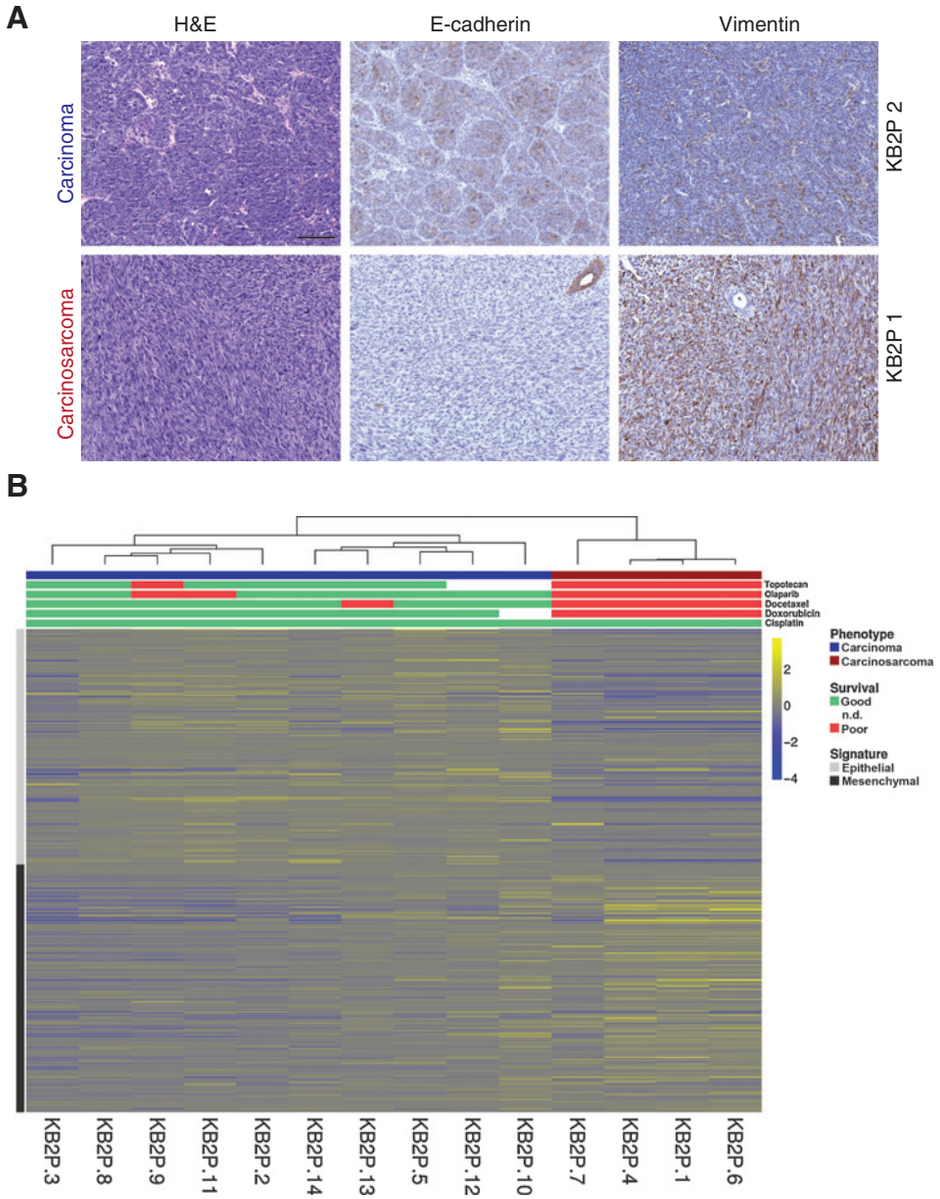

Figure 1.
Brca2$^{\Delta/\Delta}$;*p53*$^{\Delta/\Delta}$ (KB2P) carcinosarcomas are characterized by EMT-related proteins and gene-expression pattern. A, example of histology and E-cadherin and vimentin staining in a KB2P carcinoma with epithelial morphology and a KB2P carcinosarcoma with mesenchymal morphology; scale bar, 100 μm. B, the mesenchymal tumors cluster together in an unsupervised hierarchical clustering using the EMT signature genes (Supplementary Table S1). The phenotype of each tumor is determined by histology and immunohistochemical stainings for E-cadherin and vimentin (see A). Genes indicated with the gray bar are related to an epithelial cellular state and genes indicated with the black bar are higher expressed in mesenchymal cells. Red and green bars, the response to the indicated treatments for the individual donor tumors. A poor response is defined as a survival of less than 31 days after start of the treatment. Mice carrying a tumor with a good response survived more than 30 days after start of the treatment.

Results

Two main mammary tumor phenotypes are produced in *K14cre;Brca2*$^{F/F}$;*p53*$^{F/F}$ mice

To study the effect of a mesenchymal morphology on therapy response, we made use of the *K14cre;Brca2*$^{F/F}$;*p53*$^{F/F}$ mouse model (10). K14cre-mediated deletion of exon 11 of *Brca2* and exon 2–10 of *Trp53* in mammary epithelial cells (Supplementary Fig. S1) results in the development of mammary tumors with an average latency of 181 days. We used an established orthotopic transplantation model to study the response of each donor tumor to various chemotherapies (30). As described previously (10), the predominant histopathologic mammary tumor phenotype in *K14cre;Brca2*$^{F/F}$;*p53*$^{F/F}$ mice is a carcinoma with well-defined tumor cell nests. These tumors express epithelial markers such as E-cadherin and are negative for vimentin, a fibroblast and mesenchymal cell marker (Fig. 1A, top). A second phenotype present in the group of 14 *Brca2*$^{\Delta/\Delta}$;*p53*$^{\Delta/\Delta}$ (KB2P) mammary tumors used in this study, is a sarcomatoid tumor that has undergone a spindle cell metaplasia, characterized by bundles with elongated cells, absence of E-cadherin and expression of vimentin (Fig. 1A, bottom). This subtype is referred to as carcinosarcoma. In our tumor panel, we identified 10 carcinomas and four carcinosarcomas. In contrast with the clear histopathologic separation, the carcinosarcomas did not form a separate group at the genomic level when we tested aCGH data of a larger panel of *Brca2*$^{\Delta/\Delta}$;*p53*$^{\Delta/\Delta}$ carcinomas and carcinosarcomas (28) by unsupervised hierarchical clustering (Supplementary Fig. S2). Thus, these tumors do not form a clearly separate subgroup within this model for BRCA2-mutated breast cancer at the DNA level.

Because of the spindle-shaped morphology of the carcinosarcomas, we suspected that these tumors have undergone EMT after

Downloaded from cancerres.aacrjournals.org on September 22, 2019. © 2015 American Association for Cancer Research.

Published OnlineFirst December 15, 2014; DOI: 10.1158/0008-5472.CAN-14-0839

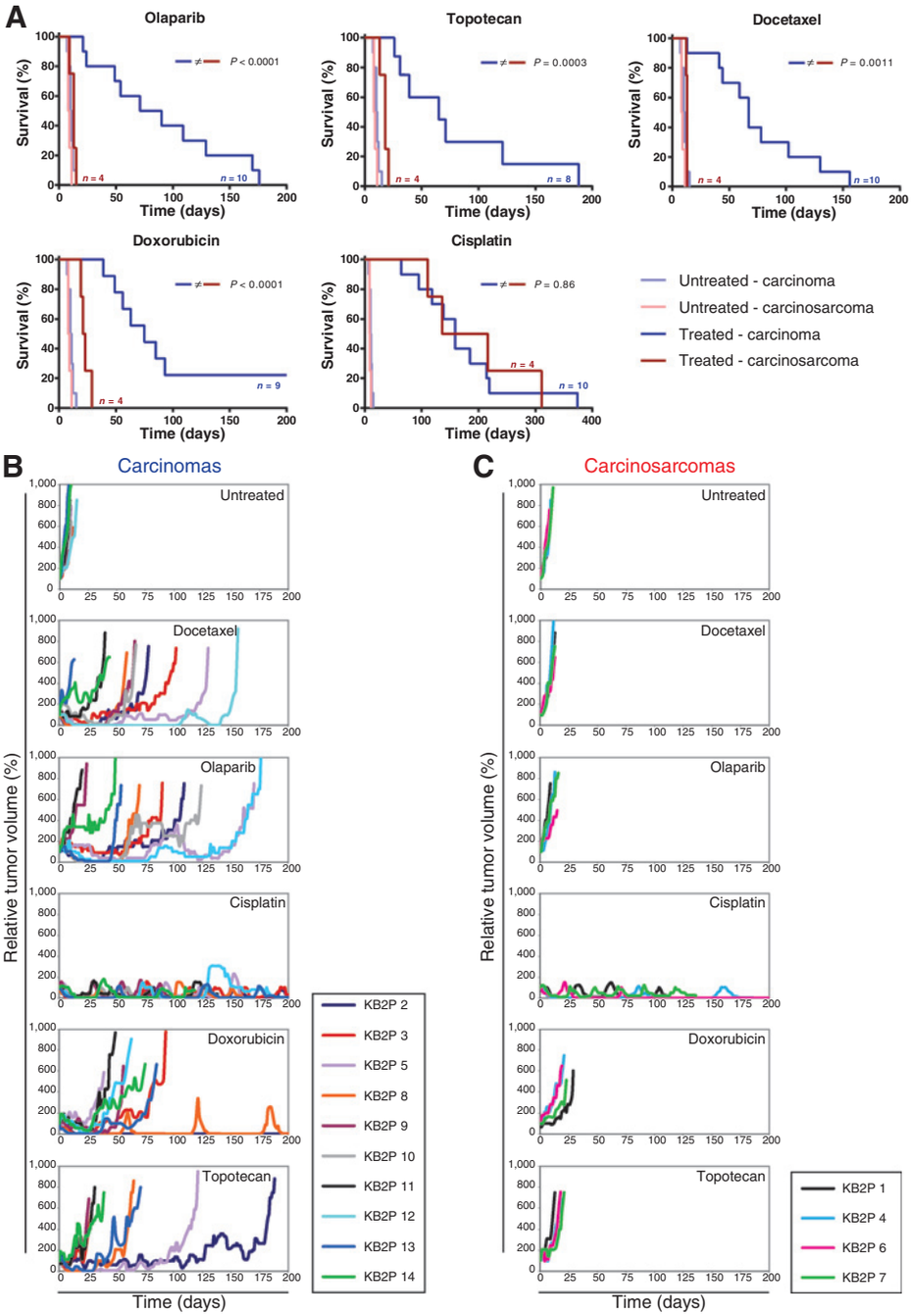

Figure 2.
Brca2$^{\Delta/\Delta}$;*p53*$^{\Delta/\Delta}$ carcinosarcomas do not respond to treatment with the PARP inhibitor olaparib, topotecan, docetaxel, or doxorubicin, but respond well to cisplatin treatment. Small tumor pieces from 14 individual KB2P donor tumors were transplanted orthotopically in wild-type syngeneic recipients. Treatment was started when the tumor reached a volume of 200 mm^3 (100%) and after relapse of the tumor to a size of 100%, another treatment cycle was given. In the Kaplan–Meier curves overall survival is shown. All mice had to be sacrificed because of a large, resistant tumor, except for the cisplatin-treated mice that were sacrificed because of cisplatin-induced cumulative toxicity. Note: the difference in time scale between cisplatin and the other treatments. The relative tumor volume of each tumor is shown in B for the carcinomas and in C for the carcinosarcomas.

the initial induction of the *Brca2* and *Trp53* mutations in an epithelial cell. To test this we, applied an EMT signature (5) to our panel of BRCA2;p53–deficient mouse mammary tumors. This signature has previously been shown to be associated with genes that are upregulated in gefitinib-resistant non–small cell lung cancers (5). In addition, the EMT index based on a subset of this signature, correlates with colorectal cancer subtypes (31). As expected, the two histologic subtypes were clearly separated in an unsupervised clustering analysis using this EMT signature (Fig. 1B). Compared with carcinomas, carcinosarcomas show higher expression of mesenchymal genes and lower expression of epithelial genes.

Brca2$^{\Delta/\Delta}$;*p53*$^{\Delta/\Delta}$ carcinosarcomas are multidrug resistant

To investigate differential drug sensitivities, we tested the response of 10 KB2P carcinomas versus 4 KB2P carcinosarcomas to the MTD of the topoisomerase I inhibitor topotecan, the microtubule-stabilizing agent docetaxel, the topoisomerase II inhibitor doxorubicin or the cross-linking agent cisplatin. As shown in Fig. 2, most KB2P carcinomas responded to all drugs,

Downloaded from cancerres.aacrjournals.org on September 22, 2019. © 2015 American Association for Cancer Research.

Published OnlineFirst December 15, 2014; DOI: 10.1158/0008-5472.CAN-14-0839

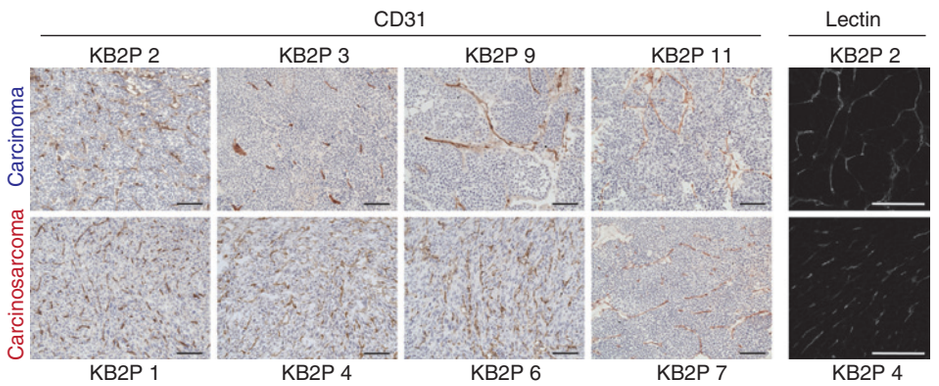

Figure 3.
Brca2$^{\Delta/\Delta}$;*p53*$^{\Delta/\Delta}$ carcinomas and carcinosarcomas are well perfused. Left, immunohistochemical staining of the endothelial cell marker CD31. Right, perfused vasculature is visualized with labeled Lycopersicon Esculentum Lectin; scale bar, 100 μm.

even though they eventually acquired resistance to olaparib, topotecan, docetaxel, and doxorubicin. In contrast, the four carcinosarcomas did not respond well to olaparib, topotecan, docetaxel, and doxorubicin, but were still sensitive to cisplatin. In Fig. 1B the response to each drug is depicted per tumor and shows that a poor response is highly correlated with a mesenchymal gene-expression profile. Carcinomas that acquired drug resistance have all retained their epithelial state, as measured by histology and gene expression (see Supplementary Fig. S3, for the olaparib-resistant tumors).

Drug delivery is not impaired in *Brca2*$^{\Delta/\Delta}$;*p53*$^{\Delta/\Delta}$ carcinosarcomas

In a mouse model for pancreatic ductal adenocarcinoma, the lack of response to gemcitabine was caused by a poor perfusion of the tumors (32). We therefore checked the presence of blood vessels in KB2P carcinomas and carcinosarcomas. Both subtypes showed blood vessels throughout the tumor (Fig. 3A). In the carcinomas, blood vessels are mainly present between the cell nests, whereas in carcinosarcomas blood vessels lay in between the tumor cells. The vessels are functional, as shown by the presence of i.v. injected, fluorescently labeled Tomato-Lectin (Fig. 3B), indicating that the drugs reach the tumor cells in both KB2P subtypes. These data are consistent with our observation that both carcinomas and carcinosarcomas respond to cisplatin.

Brca2$^{\Delta/\Delta}$;*p53*$^{\Delta/\Delta}$ carcinosarcomas can be resensitized to chemotherapy by coadministration of the Pgp inhibitor tariquidar

Each drug for which we observed primary resistance in the carcinosarcomas, is known to be transported by drug efflux transporters: olaparib (30), docetaxel (33), and doxorubicin (34) by ABCB1 (also known as Pgp) and topotecan mainly by ABCG2 (also known as BCRP; ref. 35), whereas cisplatin has no strong affinity for any efflux transporter. This suggested to us that high expression of drug efflux transporters in KB2P carcinosarcomas could have contributed to their drug resistance phenotype. In the SAM analysis, expression of *Abcb1b* (which encodes Pgp together with *Abcb1a*) was indeed higher in treatment-naïve carcinosarcomas compared with the carcinomas (Supplementary Fig. S4). We tested expression of *Abcb1a*, *Abcb1b*, and *Abcg2* in a semiquantitative manner by RT-MLPA (Fig. 4A). *Abcb1a* and *Abcb1b* were expressed at varying levels in the untreated carcinosarcomas, but three of four carcinosarcomas showed a higher expression than all carcinomas. All carcinosarcomas expressed increased levels of *Abcg2*.

To determine whether increased expression of *Abcb1a* and *Abcb1b* was causally related to the drug insensitivity, we tested the effect of the Pgp inhibitor tariquidar on therapy responses of carcinosarcomas derived from donors KB2P4 and KB2P6. Tumors were treated with tariquidar alone; olaparib, docetaxel, or doxorubicin alone; or the drug in combination with tariquidar. In addition, mice were treated with AZD2461, a novel PARP inhibitor with low affinity for Pgp (22). The effect of the combination therapy differed between the two donor tumors (Fig. 4B). KB2P4 tumors showed no effect of tariquidar on olaparib sensitivity, a small delay in outgrowth when docetaxel was combined with tariquidar, and a clear delay in tumor growth for doxorubicin plus tariquidar. All KB2P6 tumors responded well to the combination therapies of tariquidar with olaparib, docetaxel, or doxorubicin. Also, the response to AZD2461 was comparable with that of olaparib plus tariquidar. Taken together, these results show that Pgp contributed substantially to the low drug sensitivity of KB2P6 and, in the case of doxorubicin, of KB2P4.

EMT status correlates with *Abcb1b* expression in several mouse mammary tumor models

In several *in vitro* studies, EMT has been linked to resistance to various classes of drugs (4). As we observed in our KB2P mouse model, a positive correlation between an "EMT-like" gene-expression pattern and expression of *Abcb1a*, *Abcb1b*, and *Abcg2*, we wondered whether this is also the case in other mouse mammary tumor models. To obtain a continuous value for EMT, we used an EMT score based on the EMT signature. The score is calculated by subtracting the average mean-centered $\log_2$ expression of the epithelial genes from the average mean-centered $\log_2$ expression of the mesenchymal genes. We used three different gene-expression datasets from mouse mammary tumors: one that was generated at the NKI and two publicly available datasets. The first one consists of 91 mammary tumors from K14cre or WAPcre-driven mouse mammary tumor models with conditional deletion of *Trp53* alone (10) or in combination with *Cdh1* (36, 37). Similar to the KB2P model, these models develop two main histopathologic tumor subtypes: carcinoma and carcinosarcoma. The EMT score of these tumors significantly correlated with *Abcb1b* and (to a lesser extend) with *Abcb1a* and *Abcg2* (Fig. 5A). The second and third datasets are publicly available from Herschkowitz and colleagues (25) and Zhu and colleagues (26), and contain a collection of 13 and eight different genetically engineered mouse mammary

Downloaded from cancerres.aacrjournals.org on September 22, 2019. © 2015 American Association for Cancer Research.

Published OnlineFirst December 15, 2014; DOI: 10.1158/0008-5472.CAN-14-0839

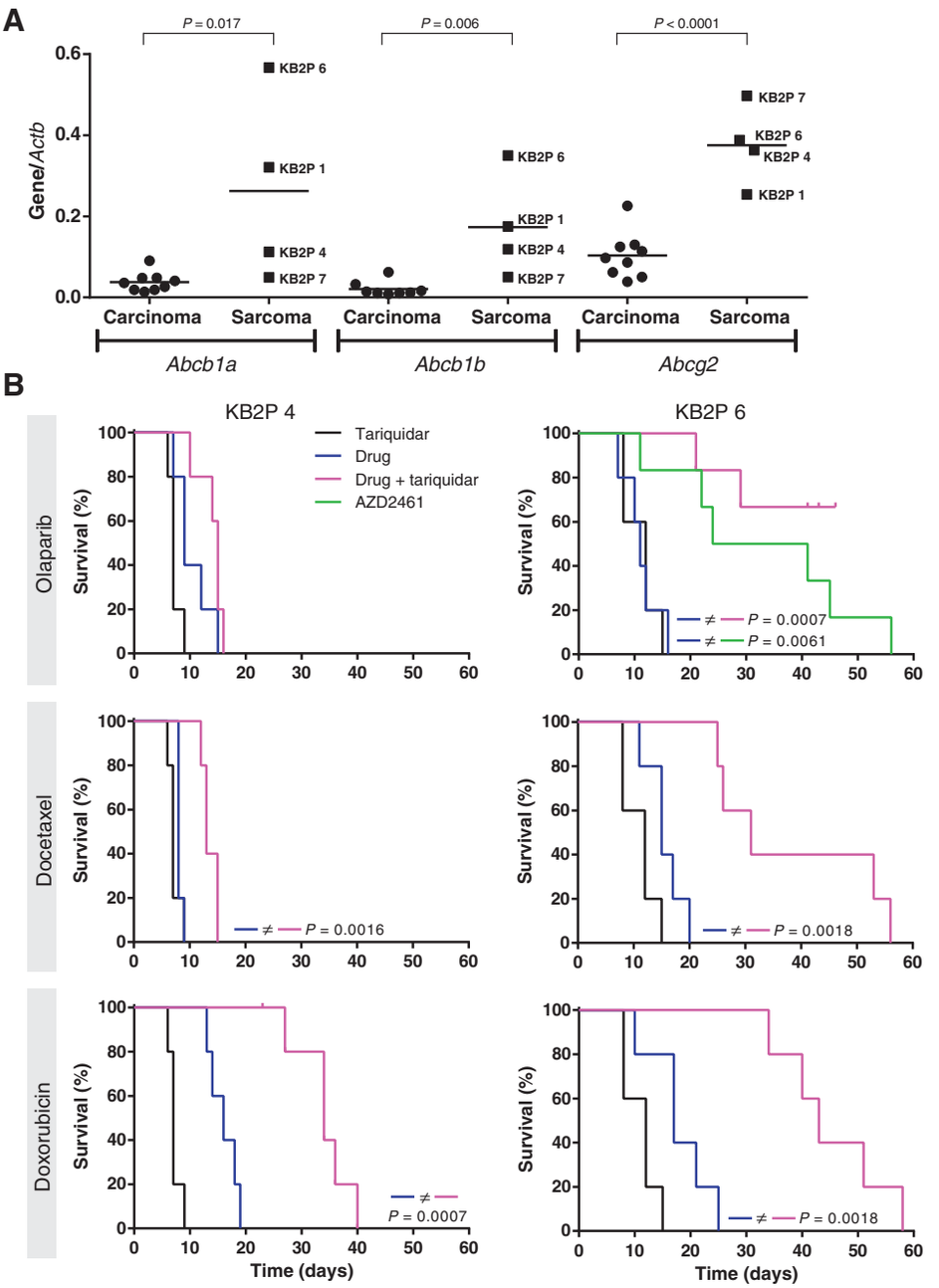

Figure 4.
Pgp contributes to multidrug resistance in *Brca2*$^{\Delta/\Delta}$;*p53*$^{\Delta/\Delta}$ carcinosarcomas. A, treatment-naïve sarcomatoid KB2P tumors have a higher expression of drug transporters *Abcb1a*, *Abcb1b* (which both encode Pgp), and *Abcg2*. Gene-expression levels were measured by RT-MLPA and normalized for *Actb* expression. For the carcinosarcomas, the expression level is indicated for each donor tumor. B, Kaplan–Meier curves showing the survival of mice bearing sarcomatoid tumors from donor KB2P4 (left) or KB2P6 (right). Treatment was started on day 0. The mice received either the Pgp inhibitor tariquidar (10 mg/kg i.p., daily), olaparib (50 mg/kg i.p., daily for 28 days), AZD2461 (100 mg/kg oral, daily for 28 days), docetaxel (25 mg/kg i.v., day 0, 7, and 14), or doxorubicin (5 mg/kg i.v., day 0, 7, and 14) or a combination of tariquidar with olaparib, docetaxel, or doxorubicin. Tariquidar was given 15 minutes before olaparib, docetaxel, or doxorubicin administration. The censored cases died because of unexpected toxicity; $n = 5$ or 6 per treatment group. The log-rank *P* values are indicated.

tumor models, respectively. Although both datasets contain mostly tumors with a low EMT score, a positive correlation between EMT score and *Abcb1b* expression was still detected (Fig. 5B and C). The lack of correlation for *Abcb1a* and *Abcg2* in these datasets is likely due to the low number of tumors with a high EMT score. Another possible explanation might be a poor sensitivity of the oligos on the expression arrays, as we have shown earlier that this affects the outcome (38).

Interestingly, in line with the KB2P data, the phenotype of *p53*$^{\Delta/\Delta}$ tumors not only correlated with *Abcb1b* expression, but also with therapy response. Mice with a *K14cre;p53*$^{\Delta/\Delta}$ (KP) carcinoma have an improved survival upon treatment with docetaxel or doxorubicin, compared with untreated control mice (Fig. 5D). KP carcinosarcomas, however, respond poorly to docetaxel and only moderately to doxorubicin. Mice with an *Abcb1a/b*$^{-/-}$ KP tumor (KPA) showed a survival time in response to docetaxel or doxorubicin, which is in between that of the KP carcinomas and carcinosarcomas (Fig. 5D, docetaxel-treated sarcomatoid KP vs. KPA $P = 0.022$; doxorubicin-treated sarcomatoid KP vs. KPA $P = 0.032$). This indicates that also in BRCA2-proficient tumors, Pgp contributes to the poor response of carcinosarcomas. Ablation of Pgp does not fully sensitize these tumors to treatment, however, which is consistent with the tariquidar combination treatments in KB2P tumors shown in Fig. 4.

Downloaded from cancerres.aacrjournals.org on September 22, 2019. © 2015 American Association for Cancer Research.

Published OnlineFirst December 15, 2014; DOI: 10.1158/0008-5472.CAN-14-0839

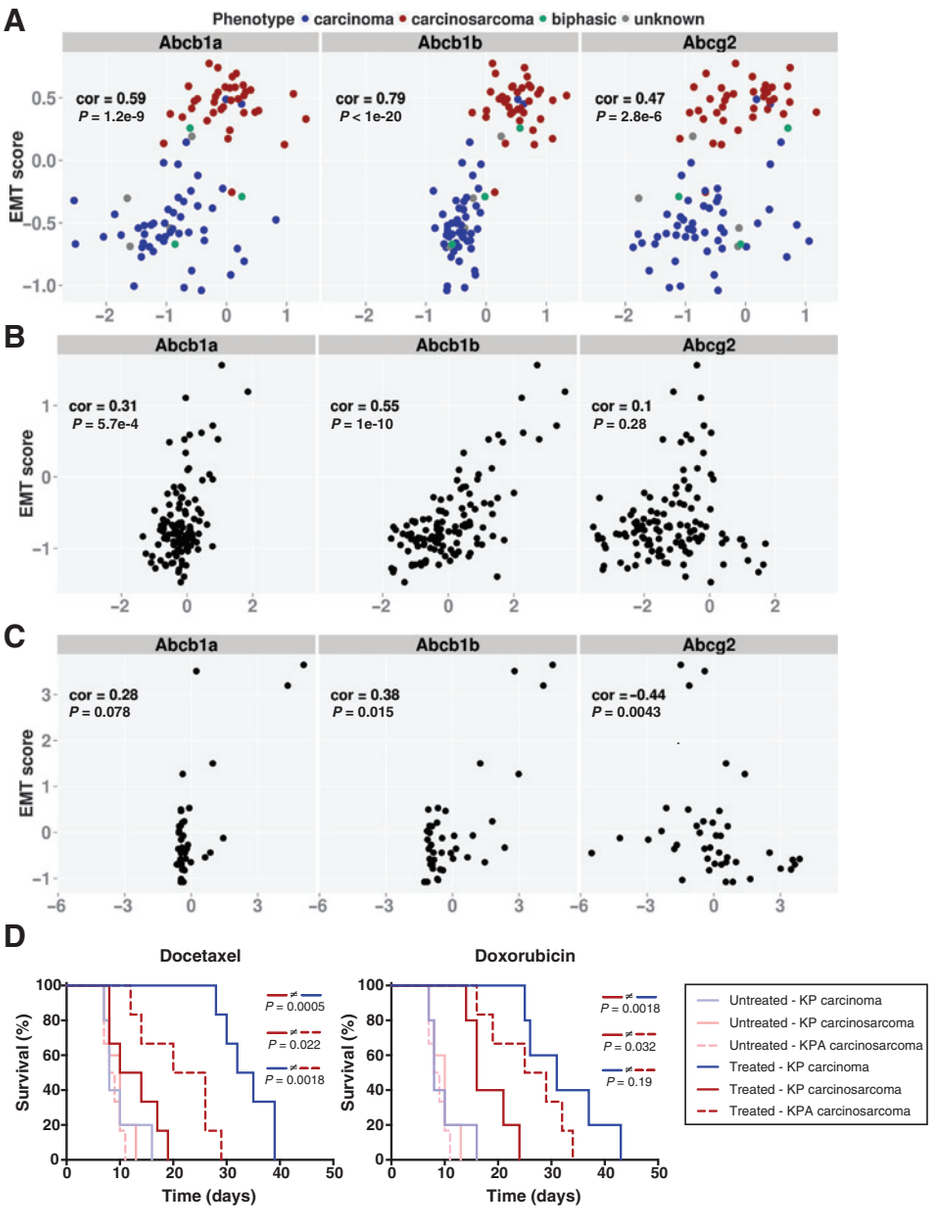

Figure 5.
EMT score correlates with *Abcb1* expression in genetically engineered mouse mammary tumor models. A–C, each plot shows the correlations between EMT score (*y*-axis) and the $\log_2$-ratio gene-expression levels (*x*-axis) of *Abcb1a*, *Abcb1b*, and *Abcg2* in three different gene-expression datasets with the Spearman correlation coefficient (cor) and *P* values of the *t* distribution. A, 91 tumors from *K14cre;p53*$^{F/F}$, *K14cre;Cdh1*$^{F/F}$*;p53*$^{F/F}$, *WAPcre;p53*$^{F/F}$, or *WAPcre;Cdh1*$^{F/F}$*;p53*$^{F/F}$ mice (Klijn; submitted for publication). The colors indicate the phenotype of each tumor as indicated in the legend. B, a publicly available dataset (GSE3165) with 108 mammary tumors from 13 different mouse models (25). C, a publicly available dataset (GSE23938) with 41 tumors from eight different mouse models (26). D, Kaplan–Meier curves showing the overall survival of mice with a p53-deficient mammary tumor (KP) of either a carcinoma or carcinosarcoma phenotype and KP carcinosarcomas that were deficient for *Abcb1a/b* (KPA), and that were treated with docetaxel, doxorubicin, or left untreated. The log-rank *P* values are indicated.

Discussion

In this study, we investigated the role of EMT in anticancer drug sensitivity in the KB2P mouse model for BRCA2-deficient breast cancer. We found that a subset of the tumors has a mesenchymal, sarcomatoid phenotype, and gene-expression profile. These BRCA2-deficient carcinosarcomas do not respond to several DNA-damaging chemotherapeutics or the PARP inhibitor olaparib, and are therefore multidrug resistant. They are not pan-resistant, because they remain highly sensitive to cisplatin, due to the irreparable deletion inactivating the *Brca2* gene, which compromises DNA repair by homologous recombination. We have previously shown that such a defect in homologous recombination by the irreparable inactivation of *Brca1* cannot be overcome by any known mechanism of resistance to cisplatin (29). We show in our KB2P model and three other mouse mammary tumor datasets that an EMT-related transcriptional profile (indicated by a high EMT score) correlates with high expression of the *Abcb1a* and *Abcb1b* genes, which both encode the drug efflux transporter Pgp. Moreover, KB2P carcinosarcomas could be sensitized to olaparib, docetaxel, and doxorubicin by the Pgp inhibitor tariquidar. Taken together, these results indicate that EMT-associated multidrug resistance is in part driven by increased activity of drug efflux transporters. Similar to the KB2P tumors, $p53^{\Delta/\Delta}$ carcinosarcomas with high *Abcb1b* expression responded poorly to docetaxel and doxorubicin, which could partially be reversed by removal of Pgp, indicating that the EMT-related resistance phenotype is independent of the BRCA2 status.

To date, only a few studies have investigated a link between EMT and drug transporter levels. Doxorubicin treatment can induce EMT in cultured breast cancer cells and upregulate efflux transporters, which is mediated by EMT transcription factors TWIST1 (39) and ZEB1 (40). Conversely, overexpression of

Downloaded from cancerres.aacrjournals.org on September 22, 2019. © 2015 American Association for Cancer Research.

Published OnlineFirst December 15, 2014; DOI: 10.1158/0008-5472.CAN-14-0839

SNAI1 in MCF7 cells results in increased Pgp levels after doxorubicin treatment (41), and in increased BCRP (ABCG2) levels (42). These studies also reported a positive correlation between SNAIL and Pgp (41), and between SNAIL and BCRP (42), respectively, in human breast cancer tissues.

In contrast with the strong evidence for a causal role of Pgp in primary and acquired resistance to chemotherapy and targeted agents in mice (20, 30, 43), the relevance of drug efflux transporters for therapy response in patients with breast cancer is still controversial. Increased Pgp mRNA or protein levels are in some, but not all, studies related to worse outcome (44). A complication in these studies is that Pgp (*ABCB1*) mRNA in tumor extracts may be derived from nontumor cells, such as macrophages, in the tumor microenvironment (43).

Over the last decades many clinical studies with transporter inhibitors have been conducted, with mostly negative results (34), and overall the impact of drug efflux transporters on patient outcome is likely to be small. This is not due to the inability of these transporters to cause resistance in real tumors. We have shown in the BRCA1-deficient mouse breast cancer model that modest levels of Pgp are sufficient to cause complete resistance to drugs used in the clinic, such as doxorubicin, docetaxel, topotecan, or olaparib (20, 30, 43). Obviously, transporter levels in human tumors are very low and transcriptional activation of the *ABCB1* gene does not easily occur in these tumors (45). Indeed, the gene needs to be linked to a strong promoter by chromosomal rearrangements for a tumor to reach sufficient levels of Pgp to acquire drug resistance (46), and this may be a rare event.

We have considered the possibility that Pgp plays a role in a small subset of breast cancer, such as metaplastic breast cancer. However, we did not find any correlation with *ABCB1* expression and a high EMT score in metaplastic tumors (Supplementary Fig. S5). This does not mean that Pgp could not play a role in some patients with acquired or secondary resistance. Unfortunately, matched samples of initially sensitive and subsequently drug-refractory tumors are hardly available from individual patients with breast cancer to address this issue.

Pgp contributes to multidrug resistance in KB2P carcinosarcomas, but our finding that KB2P4 is still insensitive to PARP inhibition and only modestly responsive to docetaxel and doxorubicin when Pgp is inhibited by tariquidar strongly suggest that other factors in the EMT program contribute as well. For example, the damage induced by PARPi and docetaxel in KB2P4 can still be compensated by another yet unknown mechanism, whereas doxorubicin-induced damage (47) is not compensated by EMT-related drug resistance in this tumor. Such EMT-associated factors could also contribute to the EMT-related drug resistance that is frequently observed in human cancer cells *in vitro*. In humans, metaplastic and claudin-low breast cancers are both associated with EMT and a triple-negative phenotype. Metaplastic breast cancers are often refractory to treatment and have a poor prognosis compared with other triple-negative breast cancers (48). The claudin-low subtype has a worse pCR rate than the basal-like group (8, 9). Several studies have demonstrated the predictive value of EMT markers (single or in combination) for prognosis and relapse-free survival (49–51), but which proteins in the EMT program eventually cause low drug sensitivity in general and to which drugs specifically still requires further investigation.

Even though several studies have shown that drug treatment, especially with doxorubicin, can induce EMT *in vitro*, we have not observed this phenomenon in any of our treated KB2P carcinomas. A possible explanation is that other resistance mechanisms are more easily activated, although it is not clear what these mechanisms might be, other than Pgp upregulation. Another option is that the carcinomas and carcinosarcomas arise from a different cell of origin, for example, a luminal or myoepithelial progenitor cell, respectively, in which K14 is expressed (10), and that they therefore do not easily switch from one type to another. This low plasticity is also illustrated by the small effect of *Snai1* or *Twist* overexpression on the phenotype of KB2P tumor cell lines *in vitro* and *in vivo* (data not shown).

Our data show that sarcomatoid HR-deficient mammary tumors respond better to cisplatin than to the PARP inhibitor olaparib. This could potentially be clinically relevant, although two major differences between human and mouse tumors must be taken into account: (i) the controversial role of drug transporters in human cancers as described above and (ii) the large, irreversible deletion of exon 11 of *Brca2* in this mouse model. Also for carcinomas, a side-by-side comparison of PARP inhibitors versus platinum drugs would be informative. In addition to BRCA1/2-mutated breast cancers also cancers with a BRCA-like CGH pattern would be useful to include. It has been shown that these are highly sensitive to platinum-based intensified chemotherapy (52) and it would be very interesting to investigate whether the same effect is achieved with PARP inhibition.

In summary, we show the usefulness of studying multidrug resistance in a realistic mouse model of BRCA2-deficient breast cancer. We found that enhanced expression of Pgp contributes to multidrug resistance associated with a sarcomatoid tumor phenotype. In addition, our data suggest that the correlation between a high EMT signature score and high expression of Pgp is a general phenomenon in mouse models of breast cancer. Pan-resistance is likely to be an accumulation of multiple mechanisms, and mouse models could be useful to unravel the different layers of resistance.

Disclosure of Potential Conflicts of Interest

No potential conflicts of interest were disclosed.

Authors' Contributions

Conception and design: J.E. Jaspers, J. Jonkers, S. Rottenberg
Development of methodology: J.E. Jaspers, S. Rottenberg
Acquisition of data (provided animals, acquired and managed patients, provided facilities, etc.): J.E. Jaspers, C. Guyader, G. Xu, S. Rottenberg
Analysis and interpretation of data (e.g., statistical analysis, biostatistics, computational analysis): J.E. Jaspers, A. Schlicker, L. Wessels, J. Jonkers, S. Rottenberg
Writing, review, and/or revision of the manuscript: J.E. Jaspers, A. Schlicker, C. Guyader, L. Wessels, P. Borst, J. Jonkers, S. Rottenberg
Administrative, technical, or material support (i.e., reporting or organizing data, constructing databases): J.E. Jaspers, W. Sol, A. Kersbergen, S. Rottenberg
Study supervision: J. Jonkers, S. Rottenberg

Acknowledgments

The authors thank Arno Velds for analyzing the aCGH data and generating Supplementary Fig. S2 and Ewa Gogola and Xaoling Liu for assistance with genotyping and Southern blotting. The authors also thank Susan Bates from the NIH (Bethesda, MD) for providing tariquidar, and Mark O'Connor from AstraZeneca for providing olaparib and AZD2461.

Downloaded from cancerres.aacrjournals.org on September 22, 2019. © 2015 American Association for Cancer Research.

Published OnlineFirst December 15, 2014; DOI: 10.1158/0008-5472.CAN-14-0839

Grant Support

This work was supported by grants from the Netherlands Organization for Scientific Research (NWO-Toptalent 021.002.104 to J.E. Jaspers; NWO-VIDI 91.711.302 to S. Rottenberg; and NWO-roadmap MCCA 184.032.303), Dutch Cancer Society (projects NKI 2007–3772, NKI 2009–4303, and NKI-2011–5220), the EU FP7 Project 260791-Eurocan-Platform, CTMM Breast Care, the Swiss National Science Foundation (grant 310030_156869), and the NKI-AVL Cancer Systems Biology Centre.

The costs of publication of this article were defrayed in part by the payment of page charges. This article must therefore be hereby marked *advertisement* in accordance with 18 U.S.C. Section 1734 solely to indicate this fact.

Received March 20, 2014; revised November 4, 2014; accepted November 16, 2014; published OnlineFirst December 15, 2014.

References

1. Borst P. Cancer drug pan-resistance: pumps, cancer stem cells, quiescence, epithelial to mesenchymal transition, blocked cell death pathways, persisters or what? Open Biol 2012;2:120066.
2. Gorre ME, Mohammed M, Ellwood K, Hsu N, Paquette R, Rao PN, et al. Clinical resistance to STI-571 cancer therapy caused by BCR–ABL gene mutation or amplification. Science 2001;293:876–80.
3. Burgess DJ, Doles J, Zender L, Xue W, Ma B, McCombie WR, et al. Topoisomerase levels determine chemotherapy response *in vitro* and *in vivo*. Proc Natl Acad Sci U S A 2008;105:9053–8.
4. Foroni C, Broggini M, Generali D, Damia G. Epithelial–mesenchymal transition and breast cancer: role, molecular mechanisms, and clinical impact. Cancer Treat Rev 2012;38:689–97.
5. Huang S, Hölzel M, Knijnenburg T, Schlicker A, Roepman P, McDermott U, et al. MED12 controls the response to multiple cancer drugs through regulation of TGF-β receptor signaling. Cell 2012;151:937–50.
6. Geyer FC, Weigelt B, Natrajan R, Lambros MBK, de Biase D, Vatcheva R, et al. Molecular analysis reveals a genetic basis for the phenotypic diversity of metaplastic breast carcinomas. J Pathol 2010;220:562–73.
7. Weigelt B, Kreike B, Reis-Filho JS. Metaplastic breast carcinomas are basal-like breast cancers: a genomic profiling analysis. Breast Cancer Res Treat 2009;117:273–80.
8. Lu S, Singh K, Mangray S, Tavares R, Noble L, Resnick MB, et al. Claudin expression in high-grade invasive ductal carcinoma of the breast: correlation with the molecular subtype. Mod Pathol 2013;26:485–95.
9. Prat A, Parker JS, Karginova O, Fan C, Livasy C, Herschkowitz JI, et al. Phenotypic and molecular characterization of the claudin-low intrinsic subtype of breast cancer. Breast Cancer Res 2010;12:R68.
10. Jonkers J, Meuwissen R, van der Gulden H, Peterse H, van der Valk M, Berns A. Synergistic tumor suppressor activity of BRCA2 and p53 in a conditional mouse model for breast cancer. Nat Genet 2001;29:418–25.
11. Gillet J-P, Varma S, Gottesman MM. The clinical relevance of cancer cell lines. J Natl Cancer Inst 2013;105:452–8.
12. Hay T, Matthews JR, Pietzka L, Lau A, Cranston A, Nygren AOH, et al. Poly (ADP-ribose) polymerase-1 inhibitor treatment regresses autochthonous Brca2/p53-mutant mammary tumors *in vivo* and delays tumor relapse in combination with carboplatin. Cancer Res 2009;69:3850–5.
13. Evers B, Schut E, van der Burg E, Braumuller TM, Egan DA, Holstege H, et al. A high-throughput pharmaceutical screen identifies compounds with specific toxicity against BRCA2-deficient tumors. Clin Cancer Res 2010;16:99–108.
14. Evers B, Drost R, Schut E, de Bruin M, van der Burg E, Derksen PWB, et al. Selective inhibition of BRCA2-deficient mammary tumor cell growth by AZD2281 and cisplatin. Clin Cancer Res 2008;14:3916–25.
15. De Plater L, Laugé A, Guyader C, Poupon M-F, Assayag F, de Cremoux P, et al. Establishment and characterisation of a new breast cancer xenograft obtained from a woman carrying a germline BRCA2 mutation. Br J Cancer 2010;103:1192–200.
16. Kortmann U, McAlpine JN, Xue H, Guan J, Ha G, Tully S, et al. Tumor growth inhibition by olaparib in BRCA2 germline-mutated patient-derived ovarian cancer tissue xenografts. Clin Cancer Res 2011;17:783–91.
17. Kriege M, Seynaeve C, Meijers-Heijboer H, Collee JM, Menke-Pluymers MBE, Bartels CCM, et al. Sensitivity to first-line chemotherapy for metastatic breast cancer in BRCA1 and BRCA2 mutation carriers. J Clin Oncol 2009;27:3764–71.
18. Lips EH, Mulder L, Hannemann J, Laddach N, Vrancken Peeters MTFD, van de Vijver MJ, et al. Indicators of homologous recombination deficiency in breast cancer and association with response to neoadjuvant chemotherapy. Ann Oncol 2011;22:870–6.
19. Tutt A, Robson M, Garber JE, Domchek SM, Audeh MW, Weitzel JN, et al. Oral poly(ADP-ribose) polymerase inhibitor olaparib in patients with BRCA1 or BRCA2 mutations and advanced breast cancer: a proof-of-concept trial. Lancet 2010;376:235–44.
20. Rottenberg S, Nygren AOH, Pajic M, van Leeuwen FWB, van der Heijden I, van de Wetering K, et al. Selective induction of chemotherapy resistance of mammary tumors in a conditional mouse model for hereditary breast cancer. Proc Natl Acad Sci U S A 2007;104:12117–22.
21. Jonkers J, Meuwissen R, van der Gulden H, Peterse H, van der Valk M, Berns A. Synergistic tumor suppressor activity of BRCA2 and p53 in a conditional mouse model for breast cancer. Nat Genet 2001;29:418–25.
22. Jaspers JE, Kersbergen A, Boon U, Sol W, van Deemter L, Zander SA, et al. Loss of 53BP1 causes PARP inhibitor resistance in Brca1-mutated mouse mammary tumors. Cancer Discov 2013;3:68–81.
23. Gautier L, Cope L, Bolstad BM, Irizarry RA. affy–analysis of Affymetrix GeneChip data at the probe level. Bioinforma Oxf Engl 2004;20:307–15.
24. Kinsella RJ, Kähäri A, Haider S, Zamora J, Proctor G, Spudich G, et al. Ensembl BioMarts: a hub for data retrieval across taxonomic space. Database 2011;2011:bar030.
25. Herschkowitz JI, Simin K, Weigman VJ, Mikaelian I, Usary J, Hu Z, et al. Identification of conserved gene expression features between murine mammary carcinoma models and human breast tumors. Genome Biol 2007;8:R76.
26. Zhu M, Yi M, Kim CH, Deng C, Li Y, Medina D, et al. Integrated miRNA and mRNA expression profiling of mouse mammary tumor models identifies miRNA signatures associated with mammary tumor lineage. Genome Biol 2011;12:R77.
27. Hennessy BT, Gonzalez-Angulo A-M, Stemke-Hale K, Gilcrease MZ, Krishnamurthy S, Lee J-S, et al. Characterization of a naturally occurring breast cancer subset enriched in epithelial-to-mesenchymal transition and stem cell characteristics. Cancer Res 2009;69:4116–24.
28. Holstege H, van Beers E, Velds A, Liu X, Joosse SA, Klarenbeek S, et al. Cross-species comparison of aCGH data from mouse and human BRCA1- and BRCA2-mutated breast cancers. BMC Cancer 2010;10:455.
29. Schouten JP, McElgunn CJ, Waaijer R, Zwijnenburg D, Diepvens F, Pals G. Relative quantification of 40 nucleic acid sequences by multiplex ligation-dependent probe amplification. Nucleic Acids Res 2002;30:e57.
30. Rottenberg S, Jaspers JE, Kersbergen A, van der Burg E, Nygren AOH, Zander SAL, et al. High sensitivity of BRCA1-deficient mammary tumors to the PARP inhibitor AZD2281 alone and in combination with platinum drugs. Proc Natl Acad Sci U S A 2008;105:17079–84.
31. Roepman P, Schlicker A, Tabernero J, Majewski I, Tian S, Moreno V, et al. Colorectal cancer intrinsic subtypes predict chemotherapy benefit, deficient mismatch repair and epithelial-to-mesenchymal transition. Int J Cancer 2014;134:552–62.
32. Olive KP, Jacobetz MA, Davidson CJ, Gopinathan A, McIntyre D, Honess D, et al. Inhibition of Hedgehog signaling enhances delivery of chemotherapy in a mouse model of pancreatic cancer. Science 2009;324:1457–61.
33. Wils P, Phung-Ba V, Warnery A, Lechardeur D, Raeissi S, Hidalgo IJ, et al. Polarized transport of docetaxel and vinblastine mediated by P-glycoprotein in human intestinal epithelial cell monolayers. Biochem Pharmacol 1994;48:1528–30.
34. Szakács G, Paterson JK, Ludwig JA, Booth-Genthe C, Gottesman MM. Targeting multidrug resistance in cancer. Nat Rev Drug Discov 2006;5:219–34.
35. Maliepaard M, van Gastelen MA, de Jong LA, Pluim D, van Waardenburg RC, Ruevekamp-Helmers MC, et al. Overexpression of the BCRP/MXR/

Downloaded from cancerres.aacrjournals.org on September 22, 2019. © 2015 American Association for Cancer Research.

Published OnlineFirst December 15, 2014; DOI: 10.1158/0008-5472.CAN-14-0839

ABCP gene in a topotecan-selected ovarian tumor cell line. Cancer Res 1999;59:4559–63.
36. Derksen PWB, Braumuller TM, van der Burg E, Hornsveld M, Mesman E, Wesseling J, et al. Mammary-specific inactivation of E-cadherin and p53 impairs functional gland development and leads to pleomorphic invasive lobular carcinoma in mice. Dis Model Mech 2011;4:347–58.
37. Derksen PWB, Liu X, Saridin F, van der Gulden H, Zevenhoven J, Evers B, et al. Somatic inactivation of E-cadherin and p53 in mice leads to metastatic lobular mammary carcinoma through induction of anoikis resistance and angiogenesis. Cancer Cell 2006;10:437–49.
38. Rottenberg S, Vollebergh MA, de Hoon B, de Ronde J, Schouten PC, Kersbergen A, et al. Impact of intertumoral heterogeneity on predicting chemotherapy response of BRCA1-deficient mammary tumors. Cancer Res 2012;72:2350–61.
39. Li Q-Q, Xu J-D, Wang W-J, Cao X-X, Chen Q, Tang F, et al. Twist1-mediated adriamycin-induced epithelial-mesenchymal transition relates to multidrug resistance and invasive potential in breast cancer cells. Clin Cancer Res 2009;15:2657–65.
40. Saxena M, Stephens MA, Pathak H, Rangarajan A. Transcription factors that mediate epithelial-mesenchymal transition lead to multidrug resistance by upregulating ABC transporters. Cell Death Dis 2011;2:e179.
41. Li W, Liu C, Tang Y, Li H, Zhou F, Lv S. Overexpression of Snail accelerates adriamycin induction of multidrug resistance in breast cancer cells. Asian Pac J Cancer Prev 2011;12:2575–80.
42. Chen W-J, Wang H, Tang Y, Liu C-L, Li H-L, Li W-T. Multidrug resistance in breast cancer cells during epithelial-mesenchymal transition is modulated by breast cancer resistant protein. Chin J Cancer 2010;29:151–7.
43. Zander SAL, Kersbergen A, van der Burg E, de Water N, van Tellingen O, Gunnarsdottir S, et al. Sensitivity and acquired resistance of BRCA1;p53-deficient mouse mammary tumors to the topoisomerase I inhibitor topotecan. Cancer Res 2010;70:1700–10.
44. Amiri-Kordestani L, Basseville A, Kurdziel K, Fojo AT, Bates SE. Targeting MDR in breast and lung cancer: discriminating its potential importance from the failure of drug resistance reversal studies. Drug Resist Updat 2012;15:50–61.
45. Faneyte IF, Kristel PM, van de Vijver MJ. Determining MDR1/P-glycoprotein expression in breast cancer. Int J Cancer 2001;93:114–22.
46. Huff LM, Lee J-S, Robey RW, Fojo T. Characterization of gene rearrangements leading to activation of MDR-1. J Biol Chem 2006;281:36501–9.
47. Pang B, Qiao X, Janssen L, Velds A, Groothuis T, Kerkhoven R, et al. Drug-induced histone eviction from open chromatin contributes to the chemotherapeutic effects of doxorubicin. Nat Commun 2013;4:1908.
48. Jung S-Y, Kim HY, Nam B-H, Min SY, Lee SJ, Park C, et al. Worse prognosis of metaplastic breast cancer patients than other patients with triple-negative breast cancer. Breast Cancer Res Treat 2010;120:627–37.
49. Iwatsuki M, Mimori K, Yokobori T, Ishi H, Beppu T, Nakamori S, et al. Epithelial-mesenchymal transition in cancer development and its clinical significance. Cancer Sci 2010;101:293–9.
50. Moody SE, Perez D, Pan T, Sarkisian CJ, Portocarrero CP, Sterner CJ, et al. The transcriptional repressor Snail promotes mammary tumor recurrence. Cancer Cell 2005;8:197–209.
51. Van Nes JGH, de Kruijf EM, Putter H, Faratian D, Munro A, Campbell F, et al. Co-expression of SNAIL and TWIST determines prognosis in estrogen receptor-positive early breast cancer patients. Breast Cancer Res Treat 2012;133:49–59.
52. Vollebergh MA, Lips EH, Nederlof PM, Wessels LF, Wesseling J, Vd Vijver MJ, et al. Genomic patterns resembling BRCA1- and BRCA2-mutated breast cancers predict benefit of intensified carboplatin-based chemotherapy. Breast Cancer Res 2014;16:R47.

Downloaded from cancerres.aacrjournals.org on September 22, 2019. © 2015 American Association for Cancer Research.

Published OnlineFirst December 15, 2014; DOI: 10.1158/0008-5472.CAN-14-0839

Cancer Research
The Journal of Cancer Research (1916–1930) | The American Journal of Cancer (1931–1940)

AACR American Association for Cancer Research

BRCA2-Deficient Sarcomatoid Mammary Tumors Exhibit Multidrug Resistance

Janneke E. Jaspers, Wendy Sol, Ariena Kersbergen, et al.

Cancer Res 2015;75:732-741. Published OnlineFirst December 15, 2014.

Updated version	Access the most recent version of this article at: doi:10.1158/0008-5472.CAN-14-0839
Supplementary Material	Access the most recent supplemental material at: http://cancerres.aacrjournals.org/content/suppl/2014/12/13/0008-5472.CAN-14-0839.DC1

Cited articles	This article cites 52 articles, 17 of which you can access for free at: http://cancerres.aacrjournals.org/content/75/4/732.full#ref-list-1
Citing articles	This article has been cited by 5 HighWire-hosted articles. Access the articles at: http://cancerres.aacrjournals.org/content/75/4/732.full#related-urls

E-mail alerts	Sign up to receive free email-alerts related to this article or journal.
Reprints and Subscriptions	To order reprints of this article or to subscribe to the journal, contact the AACR Publications Department at pubs@aacr.org.
Permissions	To request permission to re-use all or part of this article, use this link http://cancerres.aacrjournals.org/content/75/4/732. Click on "Request Permissions" which will take you to the Copyright Clearance Center's (CCC) Rightslink site.

Downloaded from cancerres.aacrjournals.org on September 22, 2019. © 2015 American Association for Cancer Research.